International Journal of Dynamics of Fluids.
ISSN 0973-1784 Volume 13, Number 1 (2017), pp. 89-112

http://www.ripublication.com

Thermophoresis Effect on a Radiating Inclined Permeable Moving Plate in the Presence of Chemical Reaction and Heat Absorption

K. Venkateswara Raju[a*] , P. Bala Anki Reddy[b] and S. Suneetha[c]

[a]Department of GEBH(Mathematics), Sree Vidyanikethan Engineering College, Tirupati--517102, India.

[b]Department of Mathematics, School of Advanced Sciences, VIT University, Vellore-632014, India.

[c]Department of Applied Mathematics, Yogi Vemana University, Kadapa-516003, Andhra Pradesh, India.*

*(*corresponding author)*

Abstract

The thermophoresis effect on the unsteady magneto-hydrodynamic mixed convection flow over an inclined permeable moving plate with the presence of thermal radiation, heat absorption and homogenous chemical reaction, subjected to variable suction is investigated. The problem is formulated in terms of non-similar equations. The equations governing the flow are transformed into a system of nonlinear ordinary differential equations by using perturbation technique. It was found that velocity distribution is increased with an increase in Soret number and in the presence of permeability, where as it shows reverse effects in the case of heat absorption coefficient, magnetic parameter, radiation parameter and chemical reaction parameter. The problem is limited to slow velocity flow of chemically reacting fluids in porous media.

Future research may consider inertia effects of porous media for relatively higher velocity flows. A very useful source of information for researchers on the subject of thermophoresis effects in porous media.

Keywords: Soret effect, MHD, Radiation, Heat absorption, Chemical reaction, Porous medium, Mixed convection, Inclined plate

INTRODUCTION

Owing to enormous practical importance and in addition to meet the requirements of the current technological desires, the convective flow problems in the cases of horizontal and vertical flat plates have been investigated quite extensively. However the boundary layer flows adjacent to inclined plates have received less attention. Combined heat and mass transfer from inclined surfaces finds numerous applications in solar energy systems, geophysics, materials processing etc.

In recent years the deposition of aerosol has a key role in the advanced technological processes. Explicitly the deposition of contaminant particle on the surface of final products has a pivotal role in the electronic industry. Mixed convection (which is a combination of natural and force convections) is one of the main factors which affect the particle deposition. Such flows occur in drying of porous solid, nuclear reactors cooled during emergency shutdown, electronic devices cooled by fans, dispersion of pollutants, solar power collectors, thermal pollution, the use of heat exchange devices, flows in the atmosphere and ocean etc. The problem being investigated is a case of mixed convection where both pressure forces and buoyant forces interact.

Magneto hydrodynamics is concerned with the mutual interaction of fluid flow and magnetic fields. Some important examples of magneto hydrodynamic flow of an electrically conducting fluid past a heated surface are MHD power generators, in creating novel power generating systems braking, plasma studies, petroleum industries, measurement of flow rates of beverages in food industry, cooling of nuclear reactors, in the prediction of space weather, the boundary- layer control in aerodynamics, damping of turbulent fluctuations in semiconductor melts in crystal growth [Chen (2004)]. Raju et al. (2014) developed about MHD convective flow through porous medium in a horizontal channel with insulated and impermeable bottom wall in the presence of viscous dissipation and joule's heating.

LIST OF SYMBOLS:

A	Suction velocity parameter	Sh	Sherwood number
B_0	Magnetic induction	T	Temperature
C	Concentration	$t^{\backslash}$	Dimensional time
C_p	Specific heat at constant pressure	T	Dimension less time
C_f	Skin friction coefficient	U_0	Scale of free stream velocity
D	Mass diffusion coefficient	$u^{\backslash},v^{\backslash}$	Dimensional velocity components
D_1	Thermal diffusion coefficient	u, v	Velocity components
$e_{b\lambda}$	Plank's function	V_0	Scale of suction velocity
F	Radiation parameter	$x^{\backslash},y^{\backslash}$	Dimensional distances along and perpendicular to the plate respectively
g	Acceleration due to gravity	x, y	Distance along and perpendicular to the plate respectively
Gr	Grashof number		**Greek Symbols**
Gm	Modified Grashof number	χ	Dimension less material parameter
K	Permeability of the porous medium	α	Inclination angle
K_c	Chemical reaction parameter	β_c	Coefficient of volumetric concentration expansion
K_λ	Absorption coefficient	β_T	Coefficient of volumetric thermal expansion
M	Magnetic field parameter	ε	Scalar constant
N	Dimensionless material parameter	η	Dimensionless normal distance
n	Dimensionless exponential index	ϕ	Dimensionless heat absorption coefficient
Nu	Nusselt number	κ	Thermal conductivity
Pr	Prandtl number	σ	Electrical conductivity
Q_0	Heat absorption coefficient	ρ	Density of the fluid
S_0	Soret number	υ	Kinematic viscosity
Re_x	Local Reynolds number		**Subscripts and Superscripts**
Sc	Schmidt number	/	Dimensional properties
Sh	Sherwood number	P	Plate
w	Wall condition	∞	Free stream condition

The goal of the thermal treatment is to cool the material to a desirable temperature before spooling or removing it. As the high temperature material emerges from a furnace or a die, is exposed to the colder ambient, therefore transient conduction process accompanied by surface heat loss is initiated. When high temperatures are encountered in the application areas, the thermal radiation effect becomes very important. High temperature plasmas, cooling of nuclear reactors, liquid metal fluids, and power generation systems are some important applications of radiative heat transfer from a surface plate to conductive fluids. There have been some studies that consider hydro magnetic radiative heat transfer flows. For instance Nath et al. (1991) obtained a set of similarity solutions for radiative-MHD stellar point explosion dynamics using shooting methods. Elbashbeshy et al. (2012) studied the effects of thermal radiation and magnetic field on an exponentially stretching surface.

Mixed convection flow and heat transfer over a continuously moving surface is applicable to many industrial fields such as hot rolling, paper production, wire drawing, glass fibre production, aerodynamic extrusion of plastic sheets, the boundary-layer along a liquid film, condensation process of metallic plate in a cooling bath and glass, and also in polymer industries. The first study of the flow field due to a surface moving with a constant velocity in a quiescent fluid was undertaken by Sakiadis (1961). Since then, other researchers [Abd El-Aziz M (2013), Javaherdeh et al. (2015)] investigated various aspects of mixed convection problems such as heat and (or) mass transfer, suction/injection, thermal radiation, MHD flow, porous media, slip flows, etc.

Convection flows with heat and mass transfer by mixed convection in a porous medium has many engineering applications such as geothermal systems, solid matrix heat exchangers, thermal insulations, oil extraction, store of nuclear waste materials, underground coal gasification, ground water hydrology, wall cooled catalytic reactors, energy efficient drying processes and natural convection in earth's crust. In a mixed convection problem, when the free stream velocity of the fluid is small and the temperature and concentration differences between the surface and ambient fluid are large then the buoyancy effects on forced convective heat and mass transfer become important. A comprehensive reviews on this topic have been given in the books by Ingham and Pop (1998, 2002) , Vafai (2007), Suneetha and Mamatha (2012) and Umamaheswar et al. (2015).

Most of the Chemical reactions involve either heterogeneous or homogeneous processes. A complex interaction lies between the homogeneous and heterogeneous reactions which is incorporated in the production and consumption of reactant species at different rates on the fluid and also on the catalytic surfaces, such are happened in fog formation and dispersion, food processing, groves of fruit trees, moisture over agricultural fields, crops damage via freezing etc. During a chemical reaction between two species, heat is also generated [Byron Bird R et al. (1992)]. Generally, the reaction rate depends on the concentration of the species itself. If the rate of reaction is directly proportional to concentration itself [Cussler (1998)], then it is said to be first order. Bala Anki Reddy (2016) revealed as the concentration decreases with increase in the value of chemical reaction parameter and solutal buoyancy parameter. The mathematical model formulated and analyzed by Srinivas et al. (2014) may be useful to clinicians, hematologists and biomedical engineers as it provides some insight to- ward the understanding the patho-physiological states of the blood flow in a narrow permeable blood vessel accounting the external magnetic field, thermal radiation and chemical reaction. Suneetha and Bala Anki Reddy (2016) focused on the impact of chemical reaction over a stretching cylinder embedded in a porous medium with lorentz forces.

An exclusive study on the influence of heat generation or absorption in moving fluids is of course being very important in complications which deal with chemical reactions and those related with separating fluids. Heat generation effects may generally alter the temperature distribution as a result the particle deposition rate in nuclear reactors, electronic chips and semiconductor wafers etc., and are reported by several researchers [Chien-Hsin (2009), Chamkha and Khaled (2001), Ibrahim et al. (2008), Noor et al.(2012), Bala Anki Reddy et al. (2016)].

The thermal diffusion has many practical applications in removing small particles from gas streams, in determining exhaust gas particle trajectories from combustion devices, air cleaning, aerosol particles sampling, micro electronics manufacturing, isotope separation and in mixtures between gases with less molecular weight (H_2, He) and medium molecular weight. Thermophoresis also called as thermo migration or thermo diffusion or the Soret effect, or the Ludwig-Soret effect. The soret effect is the dominant mass transfer mechanism in the modified chemical vapour deposition (MCVD) process as currently used in the fabrication of optical fiber performs. Thermophoretic deposition of radioactive particles is considered to be one of the important factors causing accidents in nuclear reactors. Many researches [Alam et al. (2009), Md Alamgir and Md Abdullah (2012), Reddy et al. (2010), Raju et al. (2016)] considered thermophoresis effect an inclined surface with different flow conditions.

Accordingly, the main aim of this paper is to study the thermophoresis effect on unsteady hydro magnetic mixed convection flow of a chemically reacting and heat absorbing fluid past a radiating inclined permeable moving plate in the presence of chemical reaction. The present study is structured in the following fashion. The mathematical formulation is completed in the next section. The equations governing the flow are transformed into a system of nonlinear ordinary differential equations by using perturbation technique. Then results and discussion are presented. Important results are summarized in the last section. To the best of author’s knowledge, such study has not been reported earlier in the literature.

FORMULATION OF THE PROBLEM

We have considered an unsteady two dimensional MHD flow of a viscous, incompressible, electrically conducting fluid past a semi infinite inclined moving plate embedded in a uniform porous medium. A uniform transverse magnetic field B_0 in the presence of thermal radiation and homogeneous chemical reaction is considered. It is assumed that there is no applied voltage which implies the absence of an electrical field. The transversely applied magnetic field and Reynolds number are assumed to be very small so that the induced magnetic field and the Hall Effect are negligible. x' axis is taken in the upward direction along with the flow and y' axis is taken perpendicular to it. Initially the plate is assumed to be moving with a uniform velocity u' in the direction of the fluid flow, and the free stream velocity follows the exponentially increasing small perturbation law.

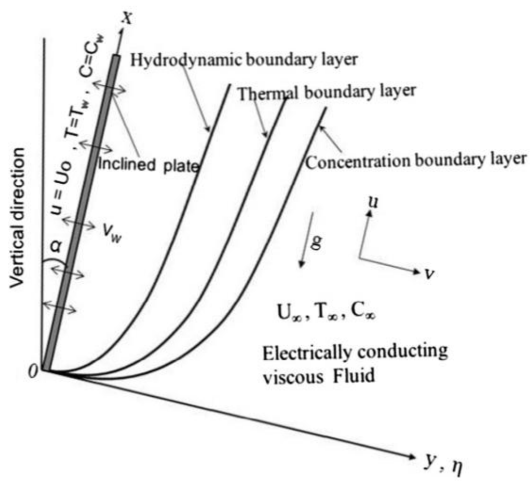

Figure 1. Schematic diagram of the physical model and coordinate system.

Besides that, it is assumed that the temperature and the concentration at the wall as well as the suction velocity are exponentially varying with time. By considering the above assumptions, the governing equations are given by

$$\frac{\partial v'}{\partial y'} = 0 \tag{1}$$

$$\frac{\partial u'}{\partial t'} + v'\frac{\partial u'}{\partial y'} = -\frac{1}{\rho}\frac{\partial p'}{\partial x'} + \upsilon\frac{\partial^2 u'}{\partial y'^2} + g\beta_T(T' - T'_\infty)\cos\alpha + g\beta_C(C' - C'_\infty)\cos\alpha - \frac{\sigma B_0^2 u'}{\rho} - \upsilon\frac{u'}{k'} \tag{2}$$

$$\frac{\partial T'}{\partial t'} + v'\frac{\partial T'}{\partial y'} = -\frac{\kappa}{\rho C_p}\frac{\partial^2 T'}{\partial y'^2} - \frac{1}{\rho C_p}\frac{\partial q_r'}{\partial y'} + \frac{Q'}{\rho C_p}\frac{\partial T'}{\partial y'} \tag{3}$$

$$\frac{\partial C'}{\partial t'}+\mathrm{v}'\frac{\partial C'}{\partial y'}=-D\frac{\partial^2 C'}{\partial y'^2}+D_1\frac{\partial^2 \mathrm{T}'}{\partial y'^2}-K_c'(\mathrm{C}'-C'_\infty) \tag{4}$$

Under the above assumptions, the appropriate boundary conditions for the distributions of velocity, temperature and concentration are given by

$$u'=u_p',T'=T'_w+\varepsilon(T'_w-T'_\infty),\mathrm{C}'=\mathrm{C}'_w+\varepsilon(C'_w-C'_\infty)\mathrm{e}^{n't'}\ \text{at}\ y'=0 \tag{5}$$

$$u'\to u'_\infty=U_0(1+\varepsilon\,\mathrm{e}^{n't'}),T'\to T'_\infty,C'\to C'_\infty\ \text{as}\ y\to\infty \tag{6}$$

It is known from Eq.(1) that the suction velocity at the plate surface is a function of time only and it is assumed in the following form

$$\mathrm{v}'=-V_0(1+\varepsilon A\,\mathrm{e}^{n't'}) \tag{7}$$

Outside the boundary layer Eq.(2) modifies as

$$-\frac{1}{\rho}\frac{\partial p'}{\partial x'}=\frac{dU'_\infty}{dt'}+\frac{\upsilon}{k'}U'_\infty+\frac{\sigma}{\rho}B_0{}^2U'_\infty \tag{8}$$

We consider a mathematical model, for an optically thin limit gray gas near equilibrium in the form given by Cramer and Pai (1973). Later Grief et al. (1971)

$$\frac{\partial q_r'}{\partial y'}=4(T'-T'_w)I \tag{9}$$

where $I=\int_0^\infty K_{\lambda w}\left(\frac{\partial e_{b\lambda}}{\partial T}\right)_w d\lambda$,

$K_{\lambda w}$ is the absorption coefficient at the wall and $e_{b\lambda}$ is the Planck's function.

By using Eqs.(7) to (9) in Eqs. (2) to (4) we get the following non-dimensional form ,

$$\frac{\partial u}{\partial t}-(1+\varepsilon Ae^{nt})\frac{\partial u}{\partial \eta}=\frac{dU_\infty}{dt}+\frac{\partial^2 u}{\partial \eta^2}+Gr\theta\cos\alpha+GmC\cos\alpha+N(U_\infty-u) \tag{10}$$

$$\frac{\partial \theta}{\partial t}-(1+\varepsilon Ae^{nt})\frac{\partial \theta}{\partial \eta}=1-\frac{\partial^2 \theta}{\partial \eta^2}-\chi\theta \tag{11}$$

$$\frac{\partial C}{\partial t}-(1+\varepsilon Ae^{nt})\frac{\partial C}{\partial \eta}=\frac{1}{Sc}\frac{\partial^2 C}{\partial \eta^2}-K_cC+S_0\frac{\partial^2 \theta}{\partial \eta^2} \tag{12}$$

where $N=M+\frac{1}{K},\quad \chi=\phi+F$

The dimension less form of the boundary conditions and become

$$u = U_P, \theta = 1 + \varepsilon A e^{nt}, \mathrm{C} = 1 + \varepsilon A e^{nt} \text{ at } \eta = 0 \tag{13}$$

$$u \to U_\infty = 1 + \varepsilon A e^{nt}, \theta \to 0, C \to 0 \text{ at } \eta \to \infty \tag{14}$$

By introducing the following non-dimensional variables and parameters

$$u = \frac{u'}{U_0}, \upsilon = \frac{\upsilon'}{V_0}, \eta = \frac{V_0 y'}{\upsilon}, U_\infty = \frac{U'_\infty}{U_0}, U_p = \frac{u'_p}{U_0}, t = \frac{t' V_0^2}{\upsilon}, \theta = \frac{T' - T'_\infty}{T'_w - T'_\infty}$$

$$C = \frac{\mathrm{C}' - C'_\infty}{\mathrm{C}'_w - C'_\infty}, \mathrm{n} = \frac{\mathrm{n}'\upsilon}{V_0^2}, K = \frac{k' V_0^2}{\upsilon^2}, \Pr = \frac{\mu C_p}{\kappa}, Sc = \frac{\upsilon}{D}, M = \frac{\sigma}{\rho}\frac{B_0^2}{V_0^2} \tag{15}$$

$$S_0 = \frac{D_1 (T'_w - T'_\infty)}{\upsilon(\mathrm{C}'_w - C'_\infty)}, K_c = \frac{K'_c \upsilon}{V_0^2}, F = \frac{4 I_1 \upsilon}{\rho C_p V_0^2}, G_r = \frac{\upsilon \beta_T g (T'_w - T'_\infty)}{U_0 V_0^2}$$

$$G_m = \frac{\upsilon \beta_C g (\mathrm{C}'_w - C'_\infty)}{U_0 V_0^2}, \phi = \frac{Q'}{\rho C_p V_0},$$

SOLUTION OF THE PROBLEM

The set of Eqs.(10) to (12) are partial differential equations which cannot be solved in closed form. However, these can be solved by reducing them into a set of ordinary differential equations using the following perturbation method. We now represent the velocity, temperature and concentration distributions in terms of harmonic and non-harmonic functions as

$$u = u_0(\eta) + \varepsilon \exp(nt) \mathrm{u}_1(\eta) + O(\varepsilon^2) + --- \tag{16}$$

$$\theta = \theta_0(\eta) + \varepsilon \exp(nt) \theta_1(\eta) + O(\varepsilon^2) + --- \tag{17}$$

$$C = C_0(\eta) + \varepsilon \exp(nt) C_1(\eta) + O(\varepsilon^2) + --- \tag{18}$$

Substituting Eqs.(16) to (18) into Eqs.(10) to (12) and equating the harmonic and non-harmonic terms, and neglecting the higher order terms of ε, we obtain the following pairs of equations of order zero and order one.

$$u_0'' + u_0' - N u_0 = -N - Gr\theta_0 \sin\alpha - GmC_0 \sin\alpha \tag{19}$$

$$u_1'' + u_1' - (N + n) u_1 = -(N + n) - A u_0' - Gr\theta_1 \sin\alpha - GmC_1 \sin\alpha \tag{20}$$

$$\theta_0'' + \Pr \theta_0' - \Pr \chi \theta_0 = 0 \tag{21}$$

$$\theta_1'' + \Pr \theta_1' - \Pr(\mathrm{n} - \chi)\theta_1 = -A \Pr \theta_0' \tag{22}$$

$$\mathrm{C}_0'' + ScC_0' - \mathrm{ScKc}\, c_0 = -ScS_0\theta_0'' \tag{23}$$

$$C_1''+S_c C_1'-(K_c S_c+S_c n)C_1=-S_c S_0 \theta_1''-AS_c C_0 \tag{24}$$

where the prime denotes differentiation with respect to η. The corresponding boundary conditions are now given by

$$u_0=U_p, u_1=0, \theta_0=1, \theta_1=1, C_0=1, C_1=1 \text{ at } \eta=0 \tag{25}$$

$$u_0=1, u_1=1, \theta_0\to 0, C_0\to 0, C_1\to 0 \text{ at } \eta\to\infty \tag{26}$$

Now by using the boundary conditions (25) and (26) and solving the set of Eqs. (18) to (24) we get the following solutions

$$u_0=1+L_{13}\exp(-m_{10}\eta)+L_{12}\exp(-m_2\eta)+L_{10}\exp(-m_6\eta) \tag{27}$$

$$u_1=\begin{pmatrix}1-L_{26}\exp(-m_{12}\eta)+L_{14}\exp(-m_{10}\eta)+L_{19}\exp(-m_8\eta)+L_{23}\exp(-m_6\eta)\\ +L_{24}\exp(-m_4\eta)+L_{25}\exp(-m_2\eta)\end{pmatrix} \tag{28}$$

$$\theta_0=\exp(-m_2\eta) \tag{29}$$

$$\theta_1=(1-L_1)\exp(-m_4\eta)+L_1\exp(-m_2\eta) \tag{30}$$

$$C_0=(1-L_2)\exp(-m_6\eta)+L_2\exp(-m_2\eta) \tag{31}$$

$$C_1=(1-L_8)\exp(-m_8\eta)+L_7\exp(-m_2\eta)+L_3\exp(-m_4\eta)+L_5\exp(-m_6\eta) \tag{32}$$

In view of the above solutions, the velocity, temperature and concentration distributions are

$$\begin{aligned}u(\eta,t)&=\left[1+L_{13}\exp(-m_{10}\eta)+L_{12}\exp(-m_2\eta)+L_{10}\exp(-m_6\eta)\right]\\&\quad+\varepsilon\exp(nt)\begin{bmatrix}1-L_{26}\exp(-m_{12}\eta)+L_{14}\exp(-m_{10}\eta)+L_{19}\exp(-m_8\eta)\\ +L_{23}\exp(-m_6\eta)+L_{24}\exp(-m_4\eta)+L_{25}\exp(-m_2\eta)\end{bmatrix}\end{aligned} \tag{33}$$

$$\theta(\eta,t)=\exp(-m_2\eta)+\varepsilon\exp(nt)\left[(1-L_1)\exp(-m_4\eta)+L_1\exp(-m_2\eta)\right] \tag{34}$$

$$\begin{aligned}C(\eta,\mathrm{t})&=\left[(1-L_2)\exp(-m_6\eta)+L_2\exp(-m_2\eta)\right]+\\&\quad\varepsilon\exp(nt)\left[(1-L_8)\exp(-m_8\eta)+L_7\exp(-m_2\eta)+L_3\exp(-m_4\eta)+L_5\exp(-m_6\eta)\right]\end{aligned} \tag{35}$$

SKIN FRICTION

Very important physical parameter at the boundary is the skin friction which is given in the non-dimensional form and derives as

$$C_f = \frac{\tau'_w}{\rho U_0 V_0} = \frac{\partial u}{\partial \eta}\Big|_{\eta=0}$$
$$= (-m_{10}L_{12} - m_2 L_{13} - m_6 L_{10}) + \varepsilon \exp(nt)(-m_{12}L_{26} - m_{10}L_{14} - m_8 L_{19} - m_6 L_{23} - m_4 L_{24} - m_2 L_{25}) \tag{36}$$

Another physical parameter including the rate of heat transfer in the form of the Nusselt number and the rate of mass transfer in the form of the Sherwood number are also derived and given below respectively

$$N_u = k' \frac{\frac{\partial T'}{\partial y'}\Big|_{y=0}}{T'_w - T'_\infty} \tag{37}$$
$$N_u \operatorname{Re}_x^{-1} = \frac{\partial \theta}{\partial \eta}\Big|_{\eta=0} = -m_2 + \varepsilon \exp(nt)(-m_4(1-L_1) - m_2 L_1)$$

$$S_h = x \frac{\frac{\partial C'}{\partial y'}\Big|_{y=0}}{C'_w - C'_\infty}$$
$$S_h \operatorname{Re}_x^{-1} = \frac{\partial C}{\partial \eta}\Big|_{\eta=0} = (-m_6(1-L_2) - m_2 L_2) + \varepsilon \exp(nt)(-m_8(1-L_7) - m_2 L_8 - m_4 L_3 - m_6 L_5) \tag{38}$$

RESULTS AND DISCUSSIONS

In this paper, the thermophoresis effect on unsteady magneto-hydrodynamic mixed convection flow over an inclined permeable moving plate in presence of thermal radiation, heat absorption and homogenous chemical reaction, subjected to the variable suction are discussed in detail through graphs from Figs. 1-22. The governing equations are having non- linear nature and have been solved by analytical method. The objective of this section is to analyze the behaviour of various involved parameters such as magnetic parameter (M), porosity parameter (K), inclined angle (α), Heat absorption coefficient (ϕ), Grashof number (Gr), modified Grashof number (Gm), radiation parameter (F), prandtl number(Pr), chemical reaction (Kc), Soret number (So), Schmidt number (Sc) on the velocity, temperature and concentration profiles. As well as the variation of skin friction, rate of heat and mass transfers in term of Nusselt and Sherwood numbers for various values of the involved parameters are shown in figures.

Figures 2 to 5 represents the velocity distribution on the parameters M, α, Gr, Gm. This shows that velocity decreases with an increase in M, α, Gr, Gm and it is observed that it finally approches around unity, when $\eta \to \infty$. An increase in M reduces the velocity. The application of a transverse magnetic field to an electrically conducting field gives rise to a resistive type of force called Lorentz force. This force has the tendency to slow down the fluid. This trend is evident from Fig.2. It can be seen in Fig.3 that the angle of inclination decreases the effect of the buoyancy force due to thermal diffusion. Consequently, the driving force to the fluid decreases as a result velocity of the fluid decreases. An increase in Gr and Gm decrease the velocity profiles. Gr signifies the relative effect of the thermal buoyancy force to the viscous hydrodynamic force in the boundary layer regime. The solutal Grashof number Gm defines the ratio of the species buoyancy force to the viscous hydrodynamic force. There is a fall in the velocity near the wall and then the velocity ascends smoothly towards unity. This trend is evident from Figs.4 and 5.

Fig. 6 represents the velocity distribution on the permeability of the porous medium K. From this, it is observed that velocity increases with an increase in K. physically, an increase in the permeability of porous medium leads the rise in the flow of fluid through it. When the holes of the porous medium become large, the resistance of the medium may be neglected. So that velocity at the insulated bottom is observed to be zero and gradually it increases as it reaches the free surface and attains a maximum unity.

The effects of Prandtl number on velocity and temperature profiles are depicted in Figs. 7 and 8. Pr encapsulates the ratio of momentum diffusivity to thermal diffusivity. Larger Pr values imply a thinner thermal boundary layer thickness and more uniform temperature distributions across the boundary layer. For Pr =1, the momentum and thermal boundary layer thicknesses, as described by Schlichting (1979), are approximately of equal extent. Smaller Pr fluids have higher thermal conductivities so that heat can diffuse away from the surface of the plate than for higher Pr fluids. Therefore, an increase in Pr leads to decrease the thickness of the thermal boundary layer, which result a uniform temperature distributions across the boundary layer. The computations show that the velocity is therefore increased as Pr rises. Fig.8 indicates that a rise in Pr substantially reduces the temperature, in the fluid saturated porous regime. The temperature decay smoothly to zero as $\eta \to \infty$, i.e. in the free stream.

Figs. 9 and 10 shows the velocity and temperature profiles for heat absorption coefficient ϕ. Fig.9 shows that increase in heat generation increases velocity. Fig 10 indicates an increase in heat generation leads decrease in temperature. Fig. 11

represents the temperature distribution on the radiation parameter F. This figure shows that the temperature decreases with an increase in F near the plate and an opposite trend is observed when $\eta > 3$ and also it approches finally around zero, when $\eta \to \infty$. Fig. 12. represents the concentration profiles for the parameter time t. This figure shows that concentration increases with an increase of time t and it is observe that it approches finally to zero, when $\eta \to \infty$.

Figures 13, 14, and 15 represents the concentration profiles for the parameters $Sc,\ Kc, S_0$. Figure 13 depicts that an increase in Sc results in a decrease in the concentration distribution, because the smaller values of Sc are equivalent to increasing the chemical molecular diffusivity. Fig.14 depicts the influence of chemical reaction effect Kc on the concentration profile. It can be seen that the concentration decreases with an increase in the values of chemical reaction parameter and hence the solutal boundary layer thickness becomes thinner. Fig. 15 presents the concentration profiles for different values of Soret number *So*. As seen from this graph that concentration of species decreases with increasing values of the Soret number.

Nusselt number Nu is represented in figures 16, 17 and 18 against radiation parameter F , heat obsorption coefficient ϕ and prandtl number $\Pr$. From these figures it is found that the nusselt number inreases with an increase in radiation parameter F, heat obsorption coefficient ϕ and prandtl number $\Pr$.

Sherwood number is studied in figures 19 and 20 against Schmidt number Sc and Soret number So.From figure 19 it is observed that sherwood number increases with an increase schmidt number Sc and also from figure 20 it is found that the sherwood number decreases with an increase of soret number So.The skin friction C_f is studied in figures 21 and 22 against Porosity parameter K and Prandtl number $\Pr$. It is seen that the skin friction C_f decreases with an increase in porosity parameter K and prandtl number $\Pr$ and also from Fig. 23 it is found that the skin friction C_f decreases with an increase of inclined angle α.

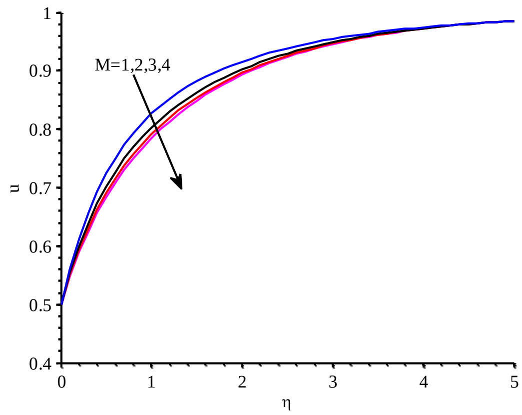

Fig.2. The velocity profile for different values of M with fixed values of

$\alpha = 15, Gr = 8, Gm = 0.1, K = 0.5, \ t = 0.5, A = 0.5, \varepsilon = 0.01, \Pr = 0.7, \phi = 0.1$

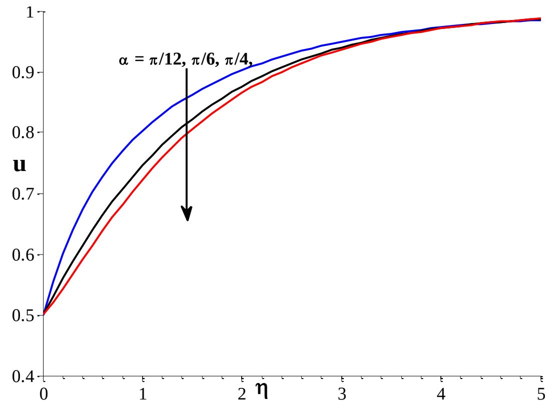

Fig.3. The velocity profile for different values of α with fixed values of

$M = 2, Gr = 8, Gm = 0.1, K = 0.5, \ t = 0.5, A = 0.5, \varepsilon = 0.01, \Pr = 0.7$

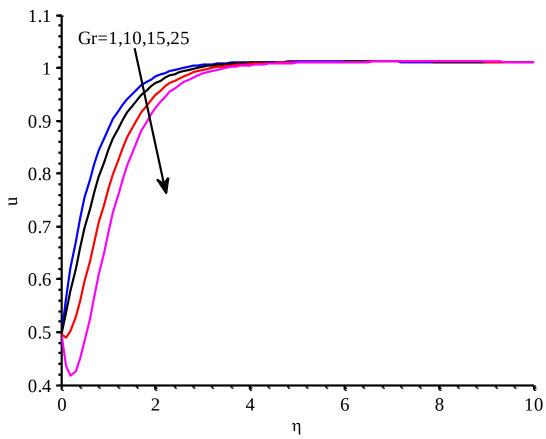

Fig 4. The velocity profile for different values of Gr with fixed values of

$M = 2, \Pr = 0.7, Gm = 0.1, \alpha = 15, \ t = 0.5, A = 0.5, \varepsilon = 0.01, K = 0.5, \phi = 0.1$

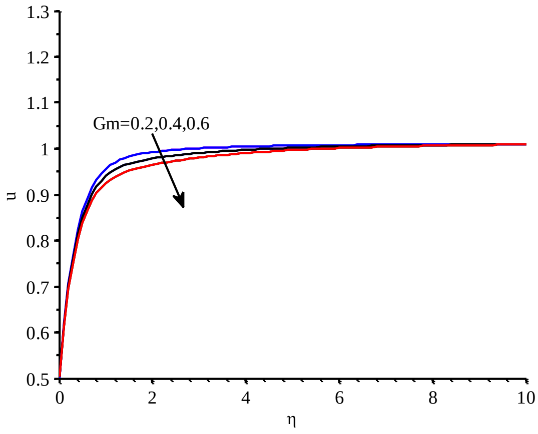

Fig. 5.The velocity profile for different values of Gm with fixed values of

$M = 2, Gr = 8, K = 0.5, \alpha = 15, \ t = 0.5, A = 0.5, \varepsilon = 0.01, \Pr = 0.7, \phi = 0.1$

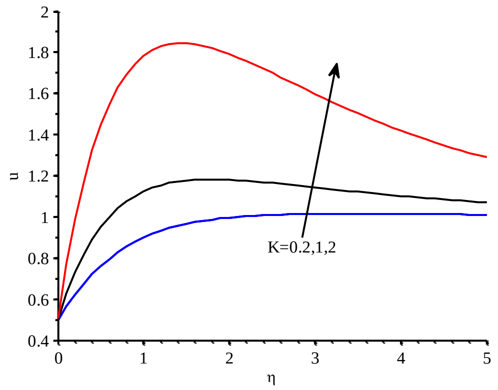

Fig. 6. The velocity profile for different values of K with fixed values of

$M = 2, Gr = 8, Gm = 0.1, \alpha = 15, \ t = 0.5, A = 0.5, \varepsilon = 0.01, \Pr = 0.7, \phi = 0.1$

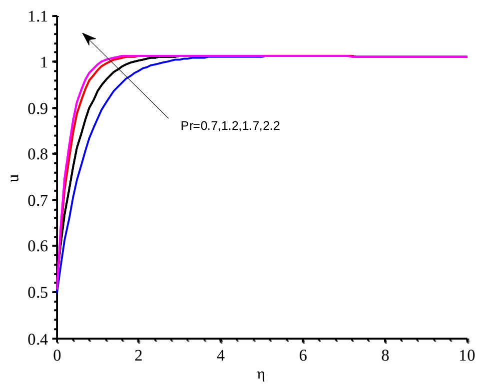

Fig.7. The velocity profile for different values of $\Pr$ with fixed values of

$M=2, Gr=8, Gm=0.1, \alpha=15,\ t=0.5, A=0.5, \varepsilon=0.01, K=0.5, \phi=0.1$

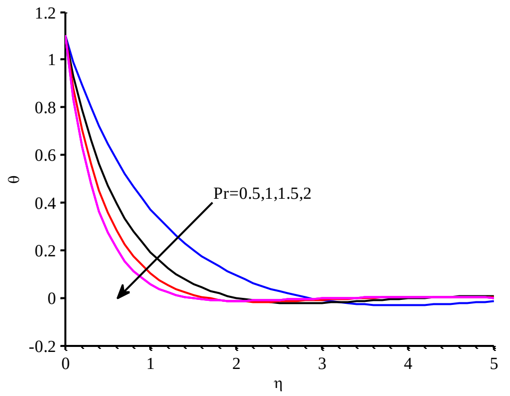

Fig. 8 The temperature profile for different values of Pr with fixed values of

$K=0.5,\ t=0.5, A=0.5, \varepsilon=0.01, \Pr=0.7, \phi=0.1,\ F=0.5$

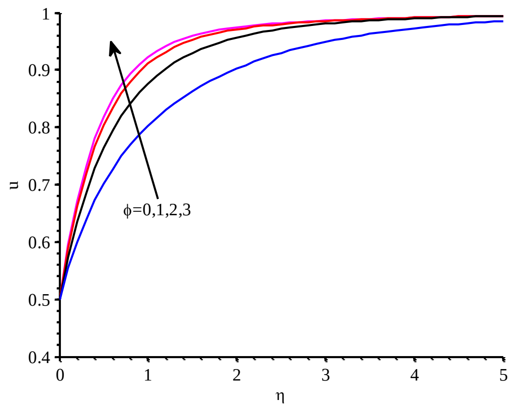

Fig. 9.The velocity profile for different values of ϕ with fixed values of

$M=2, Gr=8, Gm=0.1, K=0.5,\ t=0.5, A=0.5, \varepsilon=0.01, \Pr=0.7$

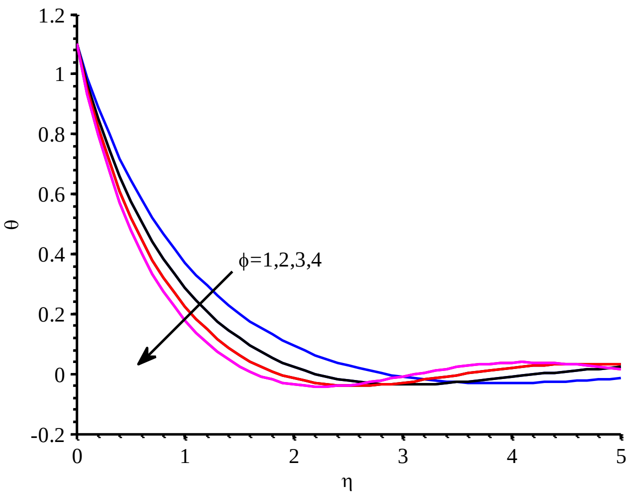

Fig. 10 The temperature profile for different values of Heat absorption coefficient ϕ with

fixed values of $K = 0.5,\ t = 0.5, A = 0.5, \varepsilon = 0.01, \Pr = 0.7, F = 0.5$

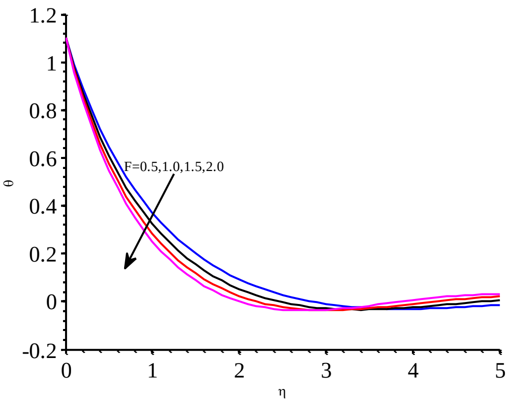

Fig. 11 The temperature profile for different values of Radiation parameter F with fixed values of $K = 0.5,\ t = 0.5, A = 0.5, \varepsilon = 0.01, \Pr = 0.7, \phi = 0.1$

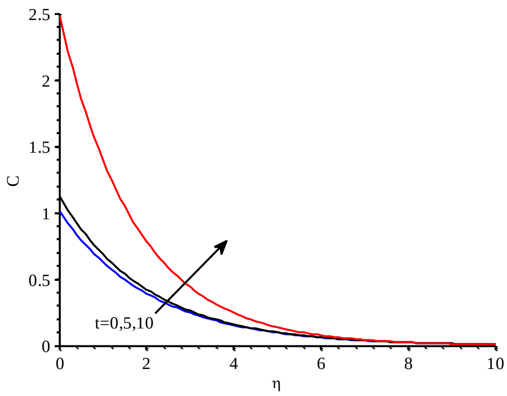

Fig.12 The concentration profile for different values of time t with fixed values of $K=0.5,\ A=0.5, \varepsilon=0.01, \Pr=0.7, \phi=0.1,\ F=0.5$

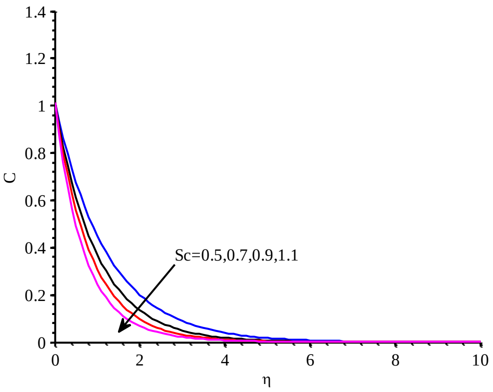

Fig.13:The concentration profile for different values of Sc with fixed values of $K=0.5,\ t=0.5, A=0.5, \varepsilon=0.01, \Pr=0.7, \phi=0.1,\ F=0.5$

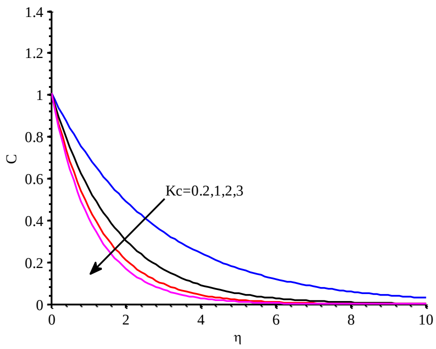

Fig. 14 The concentration profile for different values of Kc with fixed values of $K=0.5,\ t=0.5, A=0.5, \varepsilon=0.01, \Pr=0.7, \phi=0.1,\ F=0.5$

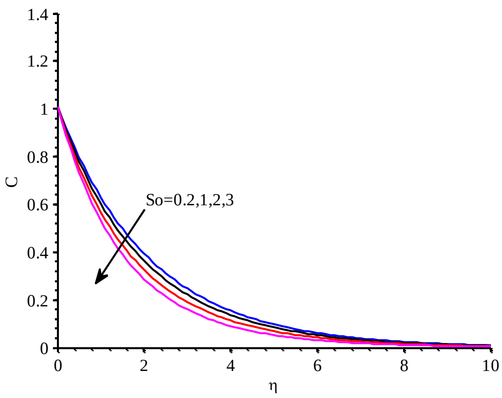

Fig.15 The concentration profile for different values of So with fixed values of $K=0.5,\ t=0.5, A=0.5, \varepsilon=0.01, \Pr=0.7, \phi=0.1,\ F=0.5$

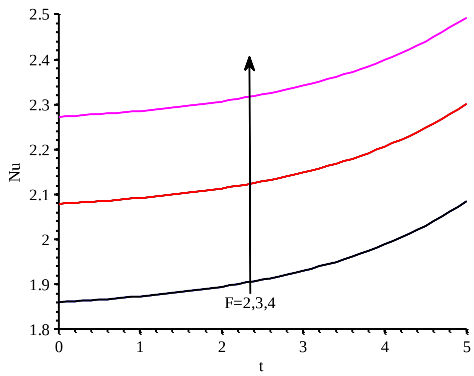

Fig. 16 The Effect of radiation parameter F on Nusselt number with fiexed values of

$$K = 0.5,\ t = 0.5, A = 0.5, \varepsilon = 0.01, \Pr = 0.7, \phi = 0.1,\ F = 0.5$$

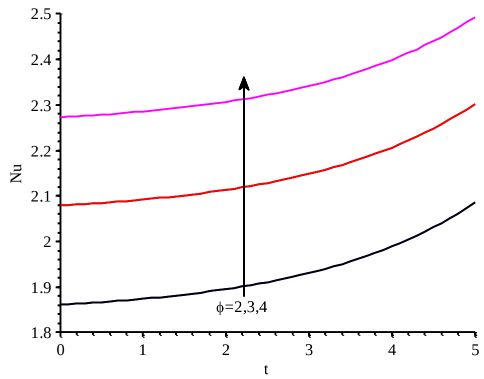

Fig.17 The Effect of heat obsorption coefficient ϕ on nusselt number with fixed values of .

$$K = 0.5,\ t = 0.5, A = 0.5, \varepsilon = 0.01, \Pr = 0.7, \phi = 0.1,\ F = 0.5$$

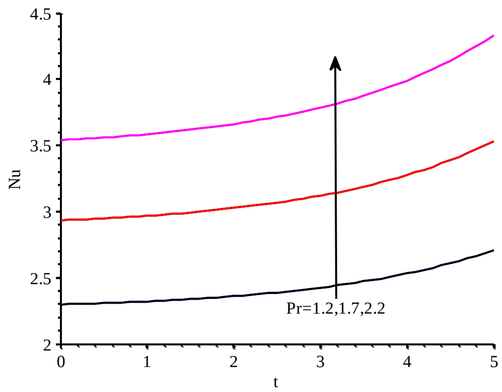

Fig. 18 The Effect of prandtl number Pr on the nusselt number with fixed values of

$$K = 0.5,\ t = 0.5, A = 0.5, \varepsilon = 0.01, \Pr = 0.7, \phi = 0.1,\ F = 0.5$$

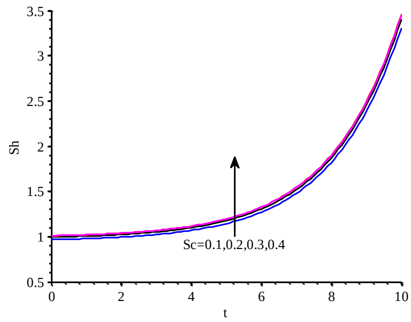

Figure 19:The Effect of Schmidt number Sc on the sherwood number with the fixed values of

$$K = 0.5,\ t = 0.5, A = 0.5, \varepsilon = 0.01, \Pr = 0.7, \phi = 0.1,\ F = 0.5$$

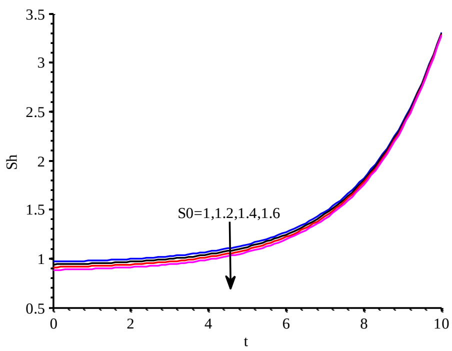

Figure 20:The Effect of Soret number So on Sherwood number with the fixed values of

$$K = 0.5,\ t = 0.5, A = 0.5, \varepsilon = 0.01, \Pr = 0.7, \phi = 0.1,\ F = 0.5$$

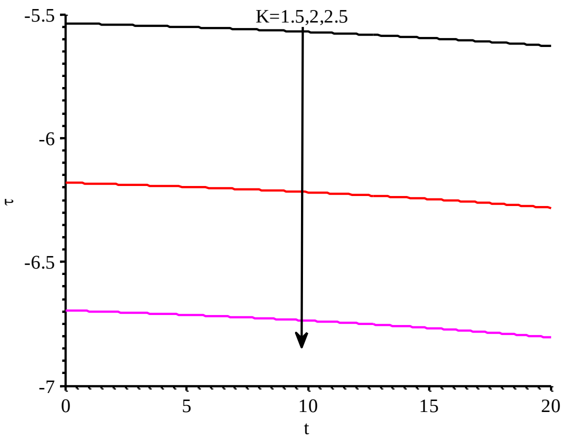

Figure 21:The Effect of Porous medium K on the skin friction with the fixed values of

$$K = 0.5,\ t = 0.5, A = 0.5, \varepsilon = 0.01, \Pr = 0.7, \phi = 0.1,\ F = 0.5$$

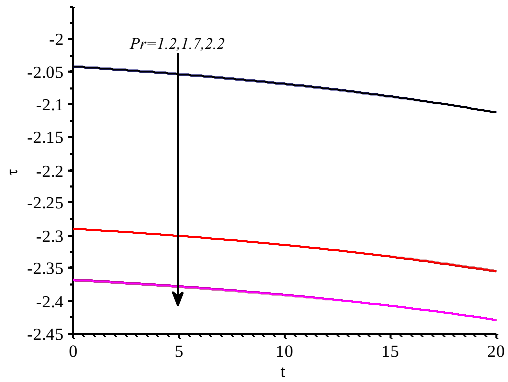

Figure 22 : The Effect of prandtal number Pr on the skin friction with the fixed values of

$$K = 0.5,\ t = 0.5, A = 0.5, \varepsilon = 0.01, \Pr = 0.7, \phi = 0.1,\ F = 0.5$$

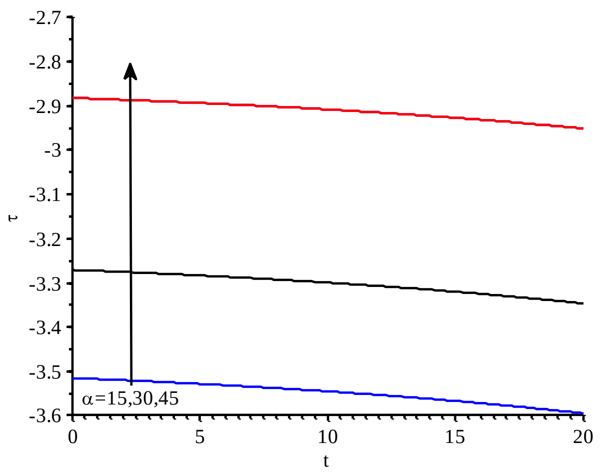

Figure 23: The effect of inclined angle α on the skin friction with the fixed values of

$$K = 0.5,\ t = 0.5, A = 0.5, \varepsilon = 0.01, \Pr = 0.7, \phi = 0.1,\ F = 0.5$$

CONCLUSIONS

Thermophoresis effect on the unsteady hydromagnetic mixed convection flow of a chemically reacting and heat absorbing fluid past a radiating inclined permeable moving plate in the presence of chemical reaction subjected to the variable suction is considered in this paper. The following is the summary of conclusions.

a) Velocity distribution is observed to decrease with an increase in magnetic parameter, inclination, where as it shows reverse effects in the case of heat absorption coefficient, in the presence of permeability, and prandtl number.

b) Temperature distribution decreases with an increase in heat absorption coefficient and prandtl number where as it decreases with an increase in radiation parameter near the plate and increases far away the plate.

c) Concentration distribution decreases as the chemical reaction parameter, Schmidt number and soret number increases.

REFERENCES

1. Abd El-Aziz M. Unsteady mixed convection heat transfer along a vertical stretching surface with variable viscosity and viscous dissipation. J Egypt Math Soc. 2013. (In press)

2. Alam MS, Rahman MM and Sattar MA. On the effectiveness of viscous dissipation and Joule heating on steady magnetohydrodynamic heat and mass

transfer flow over an inclined radiate isothermal permeable surface in the presence of thermophoresis. Commun. Nonlinear. Sci. Numer. Simul. 2009;14:2132-2143.

3. Bala Anki Reddy P. Magnetohydrodynamic flow of a casson fluid over an exponentially inclined permeable stretching surface with thermal radiation and chemical reaction. Ain Shams Engineering Journal. 2016; 7(2):593–602.(Accepted).
4. Bala Anki Reddy P, Venkateswara Raju K and Suneetha S. Effects of variable viscosity and thermal Diffusivity on MHD free convection flow along a moving vertical plate embedded in a porous medium with heat generation. Global journal of pure and applied mathematics (GJPAM). 2016; 12(3):558-562.(ISSN N0:0973-1768).
5. Byron Bird R, Warren E Stewart, Edwin Lightfoot N. Transport phenomena, John Wiley and Sons, New York, 1992.
6. Chamkha AJ, Abdul-Rahim A. Khaled. Similarity solutions for hydromagnetic heat and mass transfer by natural convection from an inclined plate with internal heat generation or absorption. Heat Mass Transfer Journal, 2001; 37: 117-123.
7. Chen CH . Heat and mass transfer in MHD flow by natural convection from a permeable, inclined surface with variable wall temperature and concentration. Acta Mech. 2004;172:219–235.
8. Chien-Hsin C .Magnetohydrodynamic mixed convection of a power-law fluid past a stretching surface in the presence of thermal radiation and internal heat generation/absorption. Int J Non-Linear Mech.2009; 44: 596–603.
9. Cramer KP and Pai SI. Magneto Fluid Dynamics for Engineers and Applied Physics. Mc Graw-Hill Book Co, New York. 1973.
10. Cussler EL. Diffusion Mass Transfer in Fluid Systems, Cambridge University Press, London, UK. 1998.
11. Elbashbeshy EMA, Emam TG, Abdelgaber KM. Effects of thermal radiation and magnetic field on unsteady mixed convection flow and heat transfer over an exponentially stretching surface with suction in the presence of internal heat generation/absorption. J Egypt Math Soc .2012;20: 215–222.
12. Grief G, Habib IS and Lin LC. Laminar convection of a radiating gas in a vertical channel. J. Fluid Mech. 1971; 45, 513–520.

13. Ibrahim FS, Elaiw AM, Bakr AA. Effect of the chemical reaction and radiation absorption on the unsteady MHD free convection flow past a semi infinite vertical permeable moving plate with heat source and suction. Communications in Nonlinear Science and Numerical Simulation. 2008; 13(6):1056–1066

14. Ingham DB and Pop I .Transport Phenomenon in Porous Media I, Pergamon, Oxford.1998.

15. Ingham DB and Pop I .Transport Phenomenon in Porous Media II, Pergamon, Oxford.2002.

16. Javaherdeh K, Mehrzad Mirzaei Nejad and Moslemi M. Natural convection heat and mass transfer in MHD fluid flow past a moving vertical plate with variable surface temperature and concentration in a porous medium. Engineering Science and Technology an International Journal. 2015;18: 423-431.

17. Md Alamgir Kabir and Md Abdullah Al Mahbub. Effects of Thermophoresis on Unsteady MHD Free Convective Heat and Mass Transfer along an Inclined Porous plate with heat Generation in Presence of Magnetic Field. Open Journal of Fluid Dynamics.2012; 120-129.

18. Nath O, Ojha SN, Takhar HS. A study of stellar point explosion in a radiative magnetohydrodynamic medium. Astrophys Space Sci .1991; 183:135–145.

19. Noor NFM, Abbasbandy S, Hashim I. Heat and mass transfer of thermophoretic MHD flow over an inclined radiate isothermal permeable surface in the presence of heat source/sink. Int J Heat Mass Trans . 2012; 55: 2122–2128.

20. Pal D, Chatterjee S . Mixed convection magnetohydrodynamic heat and mass transfer past a stretching surface in a micropolar fluid-saturated porous medium under the influence of Ohmic heating, Soret and Dufour effects. Commun Nonlin Sci Numer Simul. 2011;16:1329–1346.

21. Raju KVS, Reddy TS, Raju MC, Satyanarayana, PV, Venkataramana S .MHD convective flow through porous medium in a horizontal channel with insulated and impermeable bottom wall in the presence of viscous dissipation and joule’s heating. Ain shams Eng.J. 2014; 5(2): 543-551.

22. Raju MC, Chamkha AJ, Philip J, Varma SVK . Soret effect due to mixed convection on unsteady magnetohydrodynamic flow past a semi infinite vertical permeable moving plate in presence of thermal radiation , heat absorption and homogeneous chemical reaction. Int. J. Appl. Comput Math.

2016; 1-15.

23. Reddy NA, Varma SVK, Raju MC. Soret effects on MHD three dimensions free convection coquette flow with heat and mass transfer in presence of a heat sink**.** Int. J. Fluid Mech. 2010; 2(1):51- 60.
24. Sakiadis BC. boundary layer behaviour on continuous solid surface: I. Boundary-layer equations for two dimensional and axisymmetric flow. AIChE J .1961; 7(1):26–28.
25. Schlichting H. Boundary Layer Theory, Mac Graw Hill New York, 1979; 7 th Edition.
26. Srinivas S, Bala Anki Reddy P and Prasad BSRV . Effects of chemical reaction and thermal radiation on MHD flow over an inclined permeable stretching surface with non-uniform heat source/sink: An application to the dynamics of blood flow. Journal of Mechanics in Medicine and Biology.2014; 14 (5), 1450067.
27. Suneetha S and Mamatha B . Thermal diffusion effect on MHD heat and mass transfer flow past a porous vertical plate embedded with non-homogeneous porous medium. International Journal of Mathematical Modeling Simulation and Applications. 2012; 5(1) :52-66.
28. Suneetha S and Bala Anki Reddy P. Impact of Chemical Reaction Over A Stretching Cylinder Embedded In A Porous Medium With Lorentz Forces. Research Journal of Pharmacy and Technology.2016; 9(12): 2415-2421
29. Umamaheswar M, Varma SVK, Raju MC and Chamkha AJ. Unsteady magneto hydrodynamic free convective double –diffusive viscoelastic fluid flow past an inclined permeable plate in the presence of viscous dissipation and heat absorption. Special Topics & Reviews in Porous Media — An International Journal. 2015; 6(4): 333–342.
30. Vafai K .Handbook of Porous Media, Taylor and Francis.2007.